# Coronavirus induced primary demyelination: indications for the involvement of a humoral immune response

F. ZIMPRICH*, J. WINTER†, H. WEGE† AND H. LASSMANN*‡

*\*Research Unit for Experiment Neuropathology, Austrian Academy of Sciences, Vienna, Austria, †Institute for Virology and Immunology, University of Würzburg, Würzburg, Germany and ‡Neurological Institute, University of Vienna, Vienna, Austria*

---

ZIMPRICH F., WINTER J., WEGE H. & LASSMANN H. (1991) *Neuropathology and Applied Neurobiology* **17**, 469–484

**Coronavirus induced primary demyelination: indications for the involvement of a humoral immune response**

Coronavirus MHV-JHM infection of rodents can result in demyelinating encephalomyelitis. We analysed histological changes induced by coronavirus MHV-JHM infection in Lewis rats. Besides an acute disease (AE), chronic panencephalitis (CPE) and subacute demyelinating encephalomyelitis (SDE) were induced. These disease types were differentiated by the incubation period, the localization of lesions, the type of tissue damage and distribution of virus antigen. In AE and CPE, virus antigen was detected in neurons, astrocytes and oligodendrocytes, whereas in SDE neurons lacked virus antigen. Viral nucleocapsid protein (N) was present in the cytoplasm and the spike protein (S) was displayed on the surface of infected neural cells. However, expression of S protein relative to N protein was severely impaired in SDE lesions. Quantitative analysis of infiltrating inflammatory cells revealed that the number of macrophages and T cells were similar in lesions of AE, CPE and SDE. In contrast to that, SDE lesions contained a significantly higher number of IgG+ B cells and plasma cells. In addition active demyelinating SDE lesions displayed an enhanced IgG content and deposits of complement C9. These results indicate that virus induced primary demyelination could be a consequence of antibody mediated cytotoxicity. Furthermore, a reduction in the number of cells producing spike protein in the chronic forms of the disease indicates down-regulation of this protein, possibly mediated by anti-S antibodies.

Keywords: corona virus, MHV-JHM, spike protein, encephalitis, demyelination, remyelination, humoral immune response

---

## INTRODUCTION

Inflammatory demyelination is the main pathological change in a variety of neurological diseases of humans. Some epidemiological evidence suggests that exogenous factors, possibly viral infections, may play a role in the induction of inflammatory demyelinating diseases, such as multiple sclerosis (Waksman & Reingold, 1986). Coronavirus infections of rodents are

Correspondence to: Dr H. Lassmann, Research Unit for Experimental Neuropathology, Austrian Academy of Sciences, Neurological Institute, Schwarzspanierstr. 17, A-1090, Vienna, Austria.

models to study the pathogenesis of such diseases (Dal Canto & Rabinowitz, 1981; Kyuwa & Stohlman, 1990). Coronaviridae are enveloped viruses with a positive stranded RNA-genome (Spaan, Cavanagh & Horzinek, 1988). The spike protein S, which forms peplomers on the virion surface, and the nucleocapsid protein N are structural proteins of major importance for virus-host interactions and the immune response.

Intracerebral infection of weaning rats with JHM coronavirus results either in an acute panencephalitis (AE) or in a subacute demyelinating encephalomyelitis (SDE). The expression of these disease variants depends upon many factors such as the rat strain, the age of the animal at the time of infection and the virus strain (Cheever *et al.*, 1949; Nagashima *et al.*, 1978, 1979; Sörensen, Percy & Dales, 1980; Wege *et al.*, 1983; Koga, Wege & ter Meulen, 1984; Sörensen *et al.*, 1984; Wege, Dörries & Wege, 1984a; Watanabe, Wege & ter Meulen, 1987).

The pathogenetic mechanisms involved in tissue damage in coronavirus induced demyelinating encephalitis are still controversial. They may include a direct virus induced cytolytic effect in infected cells (Lampert, Sims & Kniazeff, 1973; Weiner, 1973), immune mediated destruction of virus infected cells or virus induced autoimmune reactions (Watanabe, Wege & ter Meulen, 1983; Wang, Stohlman & Fleming, 1990). We now present evidence that the pattern and cell tropism of virus infection closely correlates with the topographical distribution and cell specificity of tissue destruction in the CNS of infected animals. In addition, the expression of coronavirus S protein on the surface of infected cells *in vivo* as well as their reduced expression in chronic diseases and also the presence of IgG and complement C9 in actively demyelinating lesions suggests that antibodies against this viral protein may be involved in the pathogenesis of chronic demyelinating lesions in this model.

## MATERIALS AND METHODS

### Virus

The murine Corona virus strain MHV-JHM was passaged by intracerebral infection of mice and adapted to grow on Sac-cell cultures (Nagashima *et al.*, 1978; Wege *et al.*, 1984a).

### Animals

Specific pathogen free Lewis rats were obtained from the Zentralinstitut für Versuchstierzucht, Hannover, FRG. The rats were intracerebrally inoculated with 800 PFU of the MHV-JHM virus, between 3 and 8 weeks of age.

### Histology

Animals were perfused with 4% paraformaldehyde dissolved in 0.1 M phosphate buffer. Parts of the brain and spinal cord were embedded in paraffin. Paraffin sections (3 μm thick) were stained with haematoxylin & eosin, with Klüver-Barrera stain for myelin and with Bielschowsky silver impregnation for axons, or subjected to immunocytochemistry. Small tissue samples from spinal cord, brain stem and cerebellum were either processed for immune electron microscopy or post-fixed in 3% phosphate buffered glutaraldehyde, osmicated and routinely embedded in Epon for electron microscopy.

Immunohistochemical staining was performed with the avidin/biotin technique or with the alkaline phosphatase anti-alkaline phosphatase (APAAP) method as described in detail previously (Lassmann *et al.*, 1986; Vass *et al.*, 1989). Biotinylated species specific anti-mouse and

anti-rabbit sera were purchased from Amersham, UK; horse radish peroxidase labelled Avidin from Sigma, St Louis, USA, rabbit anti-mouse and APAAP complex from Dakopats, Denmark. The following primary antibodies and sera were used: a polyclonal rabbit anti JHM serum (Wege, Watanabe & ter Meulen, 1984b); mouse monoclonal antibodies against nucleo-capsid (N 556) and surface protein (S-D15 and S-E16) (Wege *et al.*, 1984a); a polyclonal rabbit serum against complement component 9 (Linington *et al.*, 1989); a rabbit serum against rat albumin (Nordic, Netherlands) and a biotinylated anti rat IgG serum (Amersham, UK) to stain plasma cells; monoclonal antibodies against glial fibrillary acidic protein (GFAP) (Boeringer Mannheim, Germany); myelin basic protein MBP (Hybtritec, USA); myelin oligodendroglial glycoprotein (MOG) (8-18-C5) and PO (a gift from Dr C. Linington). ED1 (Serotec, UK) and W3/13 (Sera-lab, UK) were applied to stain monocytes, T cells and neutrophils respectively.

For identification of the infected glial cell type (oligodendrocytes or astrocytes) we used both a morphological approach (as shown in Figure 5b,c) and a double labelling immunohisto-chemistry procedure. As a first step viral antigen was visualized using the polyclonal rabbit serum and the avidin/biotin technique. Subsequently, oligodendrocytes and astrocytes were identified on the same sections using mouse monoclonal antibodies against myelin oligo-dendroglial glycoprotein (MOG) (8-18-C5) or glial fibrillary acidic protein (GFAP) and the alkaline phosphatase anti-alkaline phosphatase (APAAP) technique.

## Immune electron microscopy

For immune electron microscopy an avidin/biotin technique was employed (Lassmann *et al.*, 1986). Sections cut with a razor blade were incubated for 8 h in each step with the following antisera, diluted in phosphate-buffered saline containing 10% fetal calf serum (FCS). Monoclonal antibodies against nucleocapsid (N556) or spike protein (S-D15 and S-E16) were used as a primary layer; sections were then incubated with biotinylated anti-mouse immuno-globulin (Amersham, UK), to which 3% rat serum was added to abolish cross reactivity completely. Horse radish peroxidase labelled avidin (Sigma, St Louis, USA) was applied in the next step and the reaction was visualized by a diaminobenzidine reagent. Sections were osmicated and embedded in Epon.

## Quantitative evaluation

Quantitative studies on virus antigens were performed in the spinal cord white matter of 14 rats from different stages of the disease. N as well as S protein expressing glial cells were evaluated in consecutive sections at least in two spinal cord levels per animal. Similarly plasma cells ($IgG^+$), macrophages ($ED1^+$) and T cells ($W3/13^+$) were counted in at least two spinal cord levels of all animals in each group. Non-parametric Mann-Whitney U test was used to analyse statistical differences in the infiltration with inflammatory cells and in the relative proportion of S expressing cells between AE, CPE and SDE.

## RESULTS

### Clinical disease

The following study was performed with tissue samples from 29 diseased Lewis rats which were selected for detailed neuropathological investigation from a total number of 400 infected Lewis

**Table 1.** Topographical distribution of inflammatory or demyelinating lesions and of virus infected cells

| Region | Inflammation/lesions | | | Virus positive cells | | |
|---|---|---|---|---|---|---|
| | AE | CPE | SDE | AE | CPE | SDE |
| Lumbar spinal cord | 6/6 | 5/5 | 9/11 | 5/6 | 5/5 | 10/11 |
| Thoracical spinal cord | 6/6 | 5/5 | 12/14 | 5/6 | 5/5 | 11/14 |
| Cervical spinal cord | 6/6 | 5/5 | 12/14 | 5/6 | 5/5 | 11/14 |
| Brain stem | 6/6 | 5/5 | 12/14 | 5/6 | 5/5 | 9/14 |
| Cerebellar white matter | 6/6 | 5/5 | 5/14 | 4/6 | 5/5 | 6/14 |
| Cerebellar cortex | 4/6 | 2/5 | 0/14 | 5/6 | 5/5 | 0/14 |
| Basal ganglia | 6/6 | 5/5 | 2/14 | 5/6 | 5/5 | 0/14 |
| Hippocampus | 5/6 | 2/5 | 1/14 | 5/6 | 4/5 | 2/14 |
| Periventricular white matter | 5/6 | 2/5 | 3/14 | 4/6 | 4/5 | 3/14 |
| Cerebral cortex | 3/6 | 2/5 | 0/14 | 5/6 | 4/5 | 0/14 |
| Meninges | 6/6 | 5/5 | 14/14 | 0/6 | 0/5 | 0/14 |

rats. Intracerebral infection of adult Lewis rats with MHV-JHM resulted in an encephalo-myelitis in 87% of the animals. The majority of the rats (66%) developed clinical signs within 8–12 days. This acute disease was characterized by ruffled fur, an ataxic, trembling gait and paralysis of fore- or hindlegs and was usually lethal. A milder and more chronic type of the disease was displayed by 21% of the rats, characterized by ruffled fur, an ataxic, trembling gait and paralysis of fore- or hindlegs several weeks to months post-inoculation. Twenty-five animals in this study were killed 8 to 210 days after infection, that is 1 to 10 days after the onset of clinical signs. Four additional animals, which recovered from the chronic disease with complete disappearance of clinical signs, were dissected 16 to 185 days after the onset of disease.

## General neuropathology

Based on the neuropathological findings and the incubation period three different disease patterns (acute encephalitis [AE], chronic panencephalitis [CPE] and subacute demyelinating encephalitis [SDE]) were distinguished. The lesional topography and the main alterations in these pathological entities are summarized in Table 1.

### Acute encephalitis

All six animals with an incubation period of less than 2 weeks showed high numbers of virus infected cells and perivascular inflammatory infiltrates distributed throughout the CNS. In addition, focal parenchymal infiltrations were present, predominantly in the grey matter of spinal cord, brain stem and hippocampus. These infiltrates consisted mainly of macrophages, lymphocytes and polymorphonuclear cells. Damaged nerve cells with either swollen and vacuolated, or dark and shrunken cytoplasm were frequently observed in the lesions. Occasionally glial nodules, composed of cells with dense and rod-like nuclei, surrounded such degenerating cells. Axon spheroids associated with secondary breakdown of myelin sheaths were observed scattered in the white matter, but primary demyelination was not seen. Activation of astrocytes visualized by thickening of their GFAP positive cellular processes was constantly seen at sites of inflammation. Albumin, IgG and complement reactivity was very low and diffusely dispersed
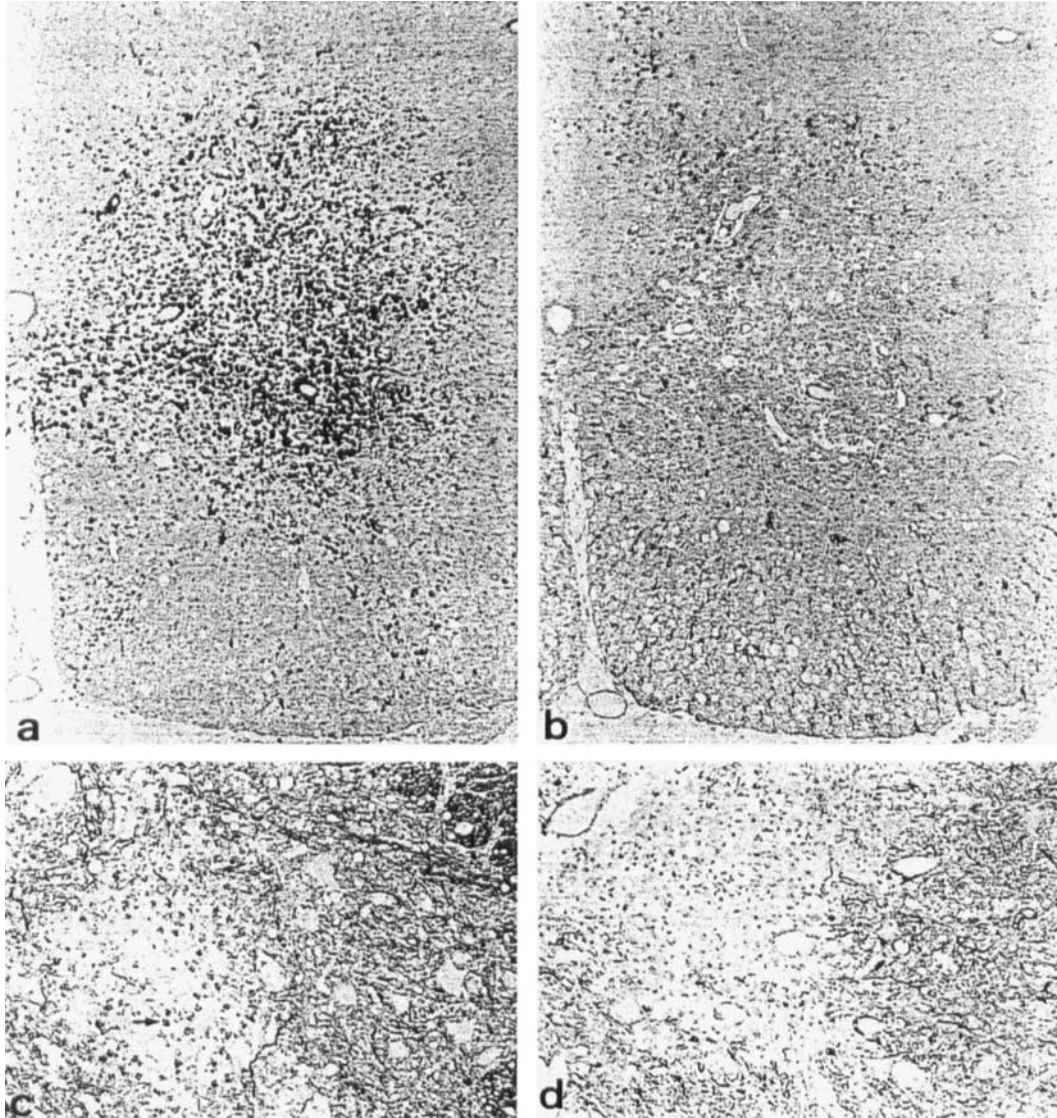
**Figure 1.** Cystic necrotic lesion of CPE in the grey matter of spinal cord. **a**, Massive infiltration with macrophages (ED1). × 70. **b**, Same area as shown in **a**, stained for viral nucleocapsid protein. Infected cells surround the necrotic lesion. × 70. **c**, **d**, the same lesion at higher magnification × 150 stained for MBP, **c**, and GFAP, **d**, degraded myelin in macrophages (arrow), **c**, complete loss of astrocytes in the lesion and gliosis in the surrounding tissue, **d**.

throughout the CNS tissue. No perivascular or parenchymal granular C9 deposits were observed.

*Chronic panencephalitis*
Similar changes to those described in AE were present in five rats with the late onset type of the disease, but they were more severe. The most conspicuous findings were symmetrically arranged necrotic lesions in the grey matter (Figure 1), most frequently encountered in the spinal cord and

brain stem. In these lesions, all structures including neurons, glial cells, axons and myelin sheaths were destroyed. Virtually all cells remaining within the lesions could be identified as inflammatory cells by the use of macrophage and lymphocyte markers (Figure 1a). In the centre of the lesions there was a complete loss of GFAP reactivity, which contrasted with the dense network of GFAP positive cells and processes in the surrounding tissue (Figure 1d).

In animals with prolonged disease we also found well demarcated areas of cystic parenchymal necrosis, especially in the grey matter of the spinal cord. Only a minor inflammatory reaction, consisting mainly of macrophages, was present within these lesions. Such areas were clearly demarcated from the adjacent tissue by a rim of gliosis.

The levels of immunoreactivity for albumin, IgG and complement C9 were very low, but in areas of pronounced inflammatory infiltration or in necrotic lesions a slightly stronger, diffuse staining was detected. No perivascular or parenchymal granular C9 deposits were observed.

Virus infected cells in AE and CPE were disseminated throughout the CNS, in grey and white matter. They were found in highest density in the grey matter of spinal cord and brain stem (Table 1). Positive cells were frequently arranged in clusters, showing a characteristic patchy appearance at low magnification. Focal, parenchymal, inflammatory infiltration was associated with these clusters. In CPE, infected cells were found to be particularly numerous in the periphery of cystic necrotic lesions (Figure 1b), whereas cells expressing virus antigen were rare within the necrotic centres.

## Subacute/chronic demyelinating encephalomyelitis

In another group of 14 animals, primary demyelinating lesions were found which were characterized by selective loss of myelin sheaths and, apart from the presence of few axon spheroids, showed relative sparing of axons. The lesions were restricted to the white matter and were mainly found in the spinal cord and brain stem and in the cerebellar and periventricular white matter. We were able to differentiate between various subtypes of demyelinating lesions, apparently reflecting different stages of lesion formation.

Early lesions were marked by a diffuse, spongiform loosening of myelin structures (Figure 2a). Astrocytes were strongly reactive for GFAP (Figure 2b). These lesions were densely infiltrated with macrophages, lymphocytes and plasma cells.

Sharply demarcated plaques, completely devoid of myelin sheaths represented a second type of lesion (Figure 2c). A massive accumulation of lipid laden macrophages was seen predominantly within the plaques (Figure 3a), whereas lymphocytes were located mainly along the actively demyelinating borders of the lesions. Almost all the cells remaining in the demyelinated plaques expressed markers specific for inflammatory cells which suggested an extensive loss of glial cells. Such a loss was also demonstrated by the reduced immunohistochemical staining for GFAP (Figure 2d) and for myelin oligodendroglia glycoprotein (MOG). In contrast to this finding, marked gliosis surrounded the lesions. Nerve cells were not involved in the pathology of SDE.

Strong albumin staining, indicating blood–brain barrier damage, was detected in most demyelinating lesions, whereas depositions of IgG and complement C9 (Figure 3b), showing diffuse and granular staining patterns, were more restricted, presumably to areas of active demyelination.

Four animals that recovered from the demyelinating disease showed peripheral, Schwann cell remyelination as early as 16 days after onset of clinical signs. Newly synthesized myelin sheaths were easily recognized with markers specific for peripheral myelin (PO protein) (Figure 2e). We observed a persistent macrophage infiltration; a few such cells were still present 150 days
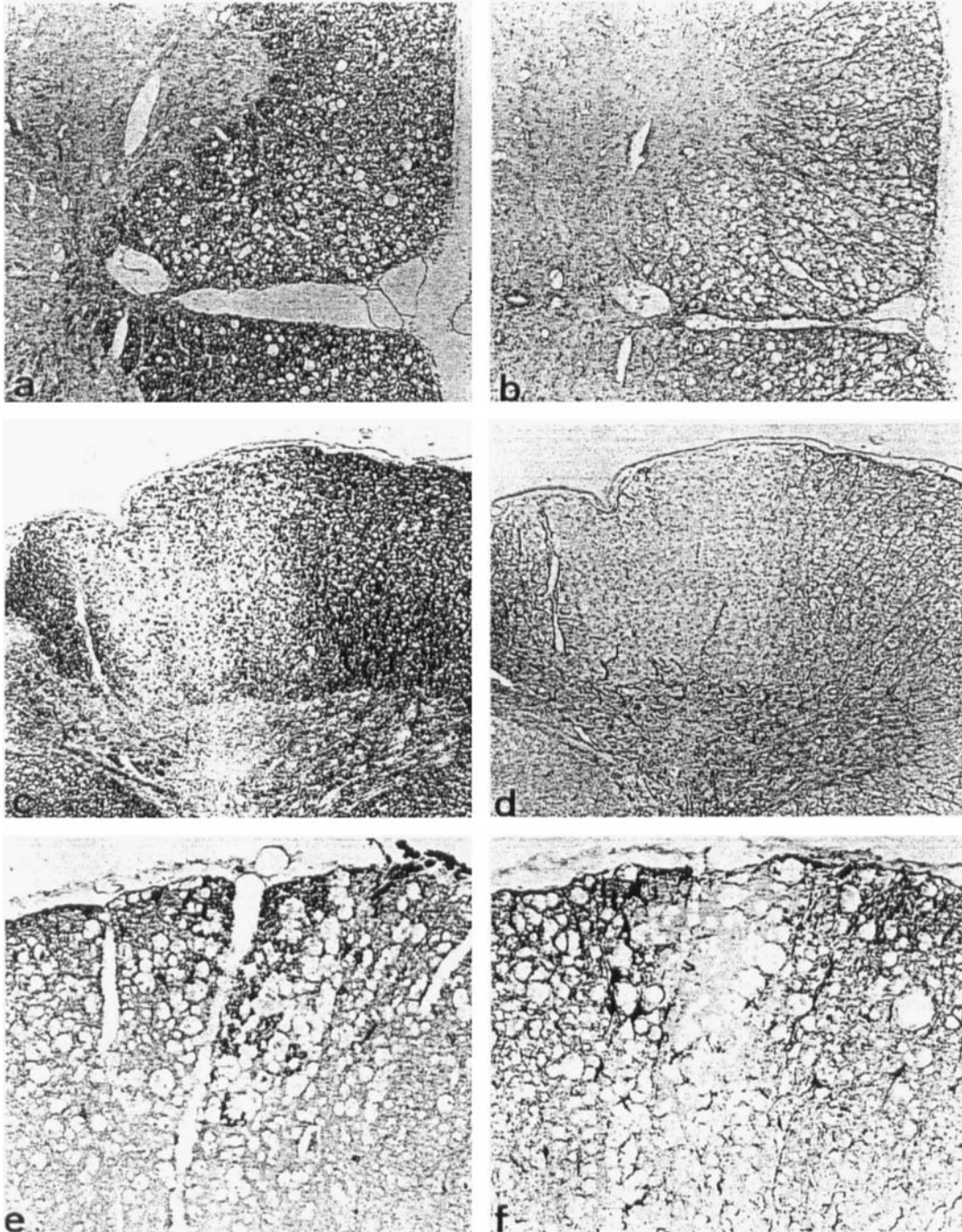
**Figure 2. a, b,** Spongiotic lesion of SDE. **a,** Spongiform vacuolation of myelin sheaths. MPB. × 70. **b,** On serial section, astrocytes are strongly reactive for GFAP. × 70: **c, d,** Demyelinated plaque. Serial sections stained for MBP and GFAP. × 70. **c,** Loss of myelin sheaths in the plaque, degraded MBP positive myelin in macrophages. **d,** Astrocytes are absent in the lesion but there is marked surrounding gliosis. **e, f,** remyelinated focus, PO positive myelin sheaths, indicating peripheral remyelination **e,** no GFAP reactivity in the focus but gliosis in the surrounding tissue. Serial sections. × 172.
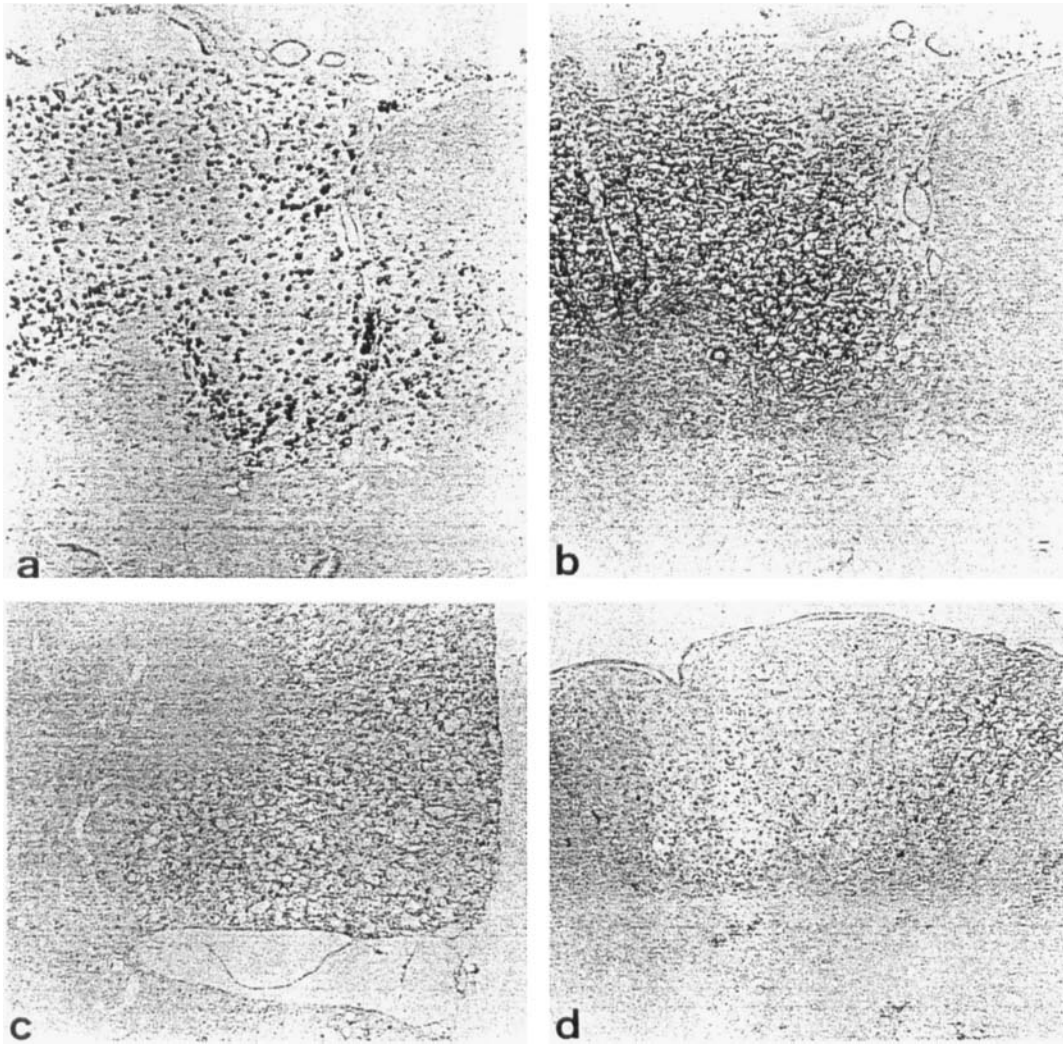
Figure 3. a, Demyelinating lesion; accumulation of macrophages within the plaque. ED1. × 70. b, Serial section. Complement C9 depositions in the demyelinating lesion. c, Even distribution of infected cells in spongiotic lesion; same area as shown in Figure 2a, b. Nucleocapsid protein. × 70. d, Infected cells surrounding the demyelinated plaque; same area as shown in Figure 2c, d. anti N. × 70.

after the disappearance of clinical disease, but we could detect no other inflammatory cells. Furthermore remyelinating foci were characterized by a loss of GFAP$^+$ astrocytes and MOG reactive oligodendrocytes in the lesions. A gliotic scar demarcated the focus from the surrounding tissue (Figure 2f).

Virus antigen in SDE was almost completely restricted to the white matter; it was most frequently detected in spinal cord and brain stem and, in a minority of cases, also in cerebellar and periventricular white matter (Table 1). In spongy lesions, infected cells were evenly distributed (Figure 3c), whereas in demyelinated plaques antigen-containing cells were concentrated
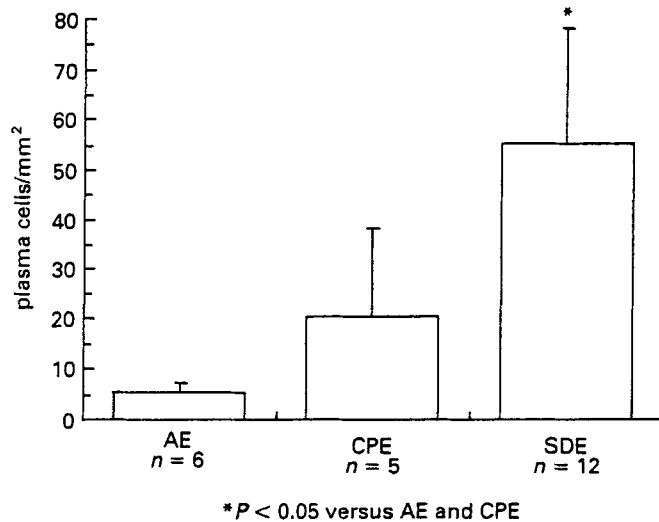
Figure 4. Histogram of infiltrated plasma cells in AE, CPE and SDE. There are significantly higher numbers of plasma cells in SDE than in AE and CPE.

in the marginal zones of active demyelination (Figure 3d). Positive cells were rare in the centre of the demyelinated plaques. Furthermore, some inactive demyelinated lesions showed no infected cells at all; in particular, we were not able to demonstrate virus antigen in remyelinated lesions.

*Quantitative comparison of inflammatory cells in AE, CPE and SDE*

There were no signficant differences in the number of infiltrating T cells and macrophages between active lesions of AE, CPE and SDE (AE: 44 (26–70) T cells/mm$^2$, 231 (98–433) macrophages/mm$^2$; CPE: 128 (46–220) T cells/mm$^2$, 697 (290–960) macrophages/mm$^2$; SDE: 147 (7–326) T cells/mm$^2$, 526 (165–1078) macrophages/mm$^2$). Infiltration with plasma cells however was significantly higher in SDE than in AE and CPE (see Figure 4).

**Identification of infected cells and subcellular distribution of virus antigen and virus particles**

Infected cells were identified by their typical morphological appearance and by double-labelling immunocytochemistry. Whereas it is comparatively simple to spot infected nerve cells and astrocytes, it is generally much more difficult to identify oligodendrocytes. However, three observations suggest that oligodendrocytes are a major infected cell type. (i) Single cells were double labelled for MOG and virus proteins. (ii) A high number of virus positive cells displayed the morphological characteristics of oligodendrocytes (e.g. chains of small round cells in the white matter). (iii) Although microglial cells are sometimes difficult to differentiate from oligodendrocytes morphologically, they are usually positive for ED1 under inflammatory conditions. ED1 positive, virus infected cells however, were extremely rare.

In AE and CPE, virus antigen was detected in nerve cells, astrocytes, oligodendrocytes and axon spheroids (Figure 5a–c). In SDE, oligodendrocytes and astrocytes contained virus antigen but neurons did not. Only rarely did we observe virus antigen in macrophages within the lesions; no virus antigen was found in inflammatory cells of perivascular cuffs.

Differences in the intracellular distribution of N and S protein were clearly visible by light microscopy. N protein was spread out diffusely in the cytoplasm of infected cells (Figure 5a–c), whereas S protein appeared as granular or linear cytoplasmic material (Figure 5e).
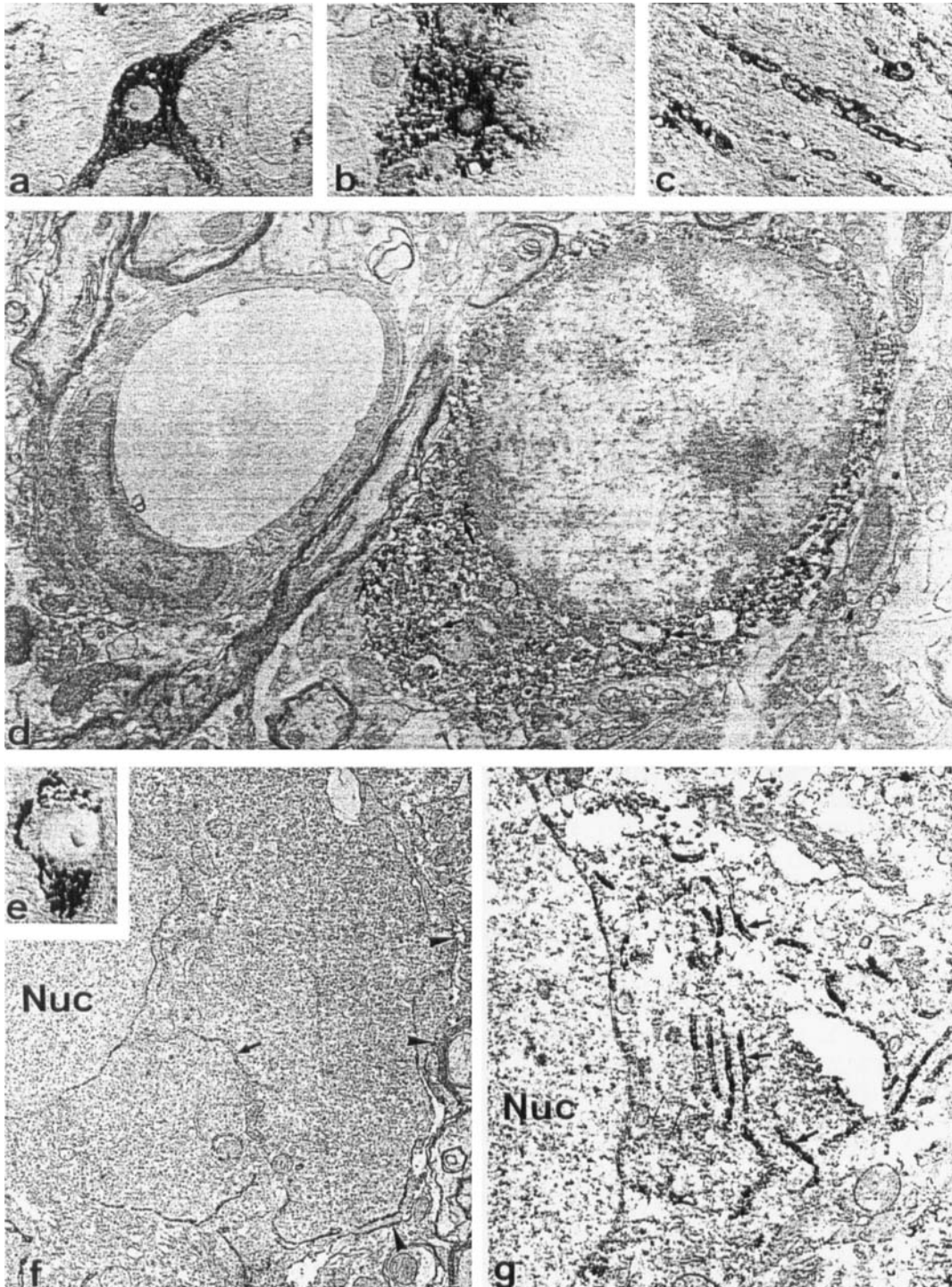
**Figure 5.** Infected **a** nerve cell, **b** astrocyte and **c** oligodendrocytes stained for JHM nucleocapsid protein showing diffuse staining of the cytoplasm. × 700. **e**, S protein shows a linear or granular staining pattern. × 700. **d**, Immune electron micrograph, cytoplasmatic patches of nucleocapsid protein (arrows). × 11 200. **f, g**, immune electron micrograph, S protein reaction product on stacks of endoplasmic reticulum (short arrows), perinuclear cisterns, vesicles and on the cell surface membrane (arrowheads). **f,** × 11 200. **g,** × 14 000.
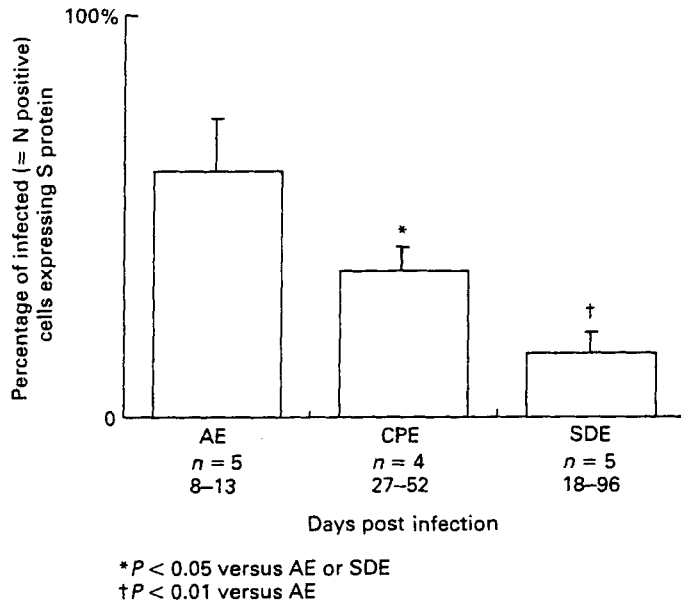
Figure 6. Histogram showing the down-regulation of spike protein in the chronic forms of the disease.

*$P < 0.05$ versus AE or SDE
†$P < 0.01$ versus AE

Immune electron microscopy demonstrated nucleocapsid protein as a granular reaction product lying free in the cytosol, leaving mitochondria, endoplasmic reticulum, Golgi apparatus, vesicles and other organelles unstained. It was either evenly filling the whole cell and all cell processes or forming focal aggregations (Figure 5d).

S protein, in contrast, was strictly associated with membranes, showing a patchy or continuous linear staining pattern. Reaction product was found on perinuclear cisterns, endoplasmic reticulum and on vesicles. In addition, smaller amounts of S protein were also expressed on the extracellular side of the surface membranes of infected cells (Figure 5f,g).

Intracytoplasmic accumulations of electron dense material were observed by conventional electron microscopy, corresponding in structure and localization to nucleocapsid protein or core particles. Although, in adjacent paraffin embedded sections, up to 700 virus positive cells/$mm^2$ were counted, only two or three of these cells in the same area actually contain morphologically recognizable virus particles. The 100 nm, round virus particles were always found within vesicles of cells with an otherwise normal appearance. No virus particles were found in ballooned or pyknotic, degenerating cells.

## Expression of nucleocapsid and spike protein in AE, CPE and SDE

When quantifying the extent of the infection, we also compared, on consecutive paraffin sections, the number of cells stained positively for N or S protein (Figure 6). Although there were always fewer cells which expressed detectable levels of S protein than nucleocapsid protein, the degree varied in different animals and lesion types. In AE an average of 60% (between 40 and 74%) of N positive cells contain S protein. In SDE, however, a significantly lower proportion of cells ($P < 0.01$ in Mann-Whitney U test) was stained with S specific antibodies, i.e. only about 15% (between 5 and 30%) of N reactive cells. The values of relative S expression in CPE (between 29% and 41%) were significantly lower than in AE ($P < 0.05$) but significantly higher than in SDE ($P < 0.05$).

## DISCUSSION

This study gives a detailed neuropathological description of changes following infection of rats with a neurotropic coronavirus. An array of lesions, which differ in complexity, was observed. Some evidence was obtained that the antiviral immune response may contribute to primary demyelination and virus persistence.

Animals developing a fatal disease within less than 2 weeks showed the changes of AE. Those rats with a milder, later onset of disease, however, revealed two different types of lesion. In the majority of animals, demyelinating lesions of SDE were found, but in one third of the rats, a chronic panencephalitis with tissue necrosis in both the grey and white matter was observed. Although previous authors describe neuropathological changes of AE and SDE in JHM virus infected rats (Cheever et al., 1949; Nagashima et al., 1978, 1979; Sörensen et al., 1980; Wege et al., 1984b; Koga et al., 1984), the occurrence of late onset CPE has not been reported so far.

The initial inflammatory changes appearing in CPE are ubiquitous perivascular cuffs in grey and white matter, similar to AE. Focal parenchymal accumulations of inflammatory cells and necrotic areas with destruction of normal CNS structures probably reflect later stages. Finally, lesions develop into cystic necrotic foci with very little remaining inflammation. Thus, this disease type differs from AE, which usually leads to death within 1 or 2 days in that it has a later onset and a milder and prolonged disease course. This prolonged disease course allows sufficient time for fully developed necrotic lesions to be formed or even for the inflammatory component to be resolved.

In SDE, different variants of demyelinating lesion were found. Diffuse spongiotic white matter changes, similar to those mentioned by Nagashima et al. (1978), apparently constitute initial stages of demyelination. The well demarcated demyelinated plaques presumably represent older lesions, in which most axons have lost their myelin sheaths and myelin degradation products are found in phagocytes. An interesting observation was the extensive, almost complete loss of both oligodendrocytes and astrocytes in these lesions. There have been no reports of the extent of glial and particularly astroglial cell destruction. Previous investigators considered degenerating cells in lesions to be mainly oligodendrocytes (Lampert et al., 1973; Nagashima et al., 1978, 1979).

Remyelination of SDE lesions was reported to be mainly of the CNS type and occasionally also of the PNS type (Herndon et al., 1975; Nagashima et al., 1979; Wege et al., 1984b; Watanabe et al., 1987). We observed in this study extensive Schwann cell invasion and peripheral remyelination. As shown in demyelinating models based on intoxication, CNS remyelination cannot occur unless sufficient oligodendrocytes and probably also astrocytes are present (Ludwin, 1980; Blakemore & Crang, 1988). In addition, it is known that invasion of Schwann cells is restricted to areas with astrocytic damage and destruction of the glial limiting membrane (Blakemore, 1978; Blakemore, Crang & Curtis, 1986). Thus the observed destruction of both oligodendrocytes and astrocytes in SDE lesions might be the reason for peripheral remyelination.

Virus antigen was demonstrated in nerve cells, oligodendrocytes and astrocytes in panencephalitic lesions. In SDE lesions, only oligodendrocytes and astrocytes displayed virus antigen. Previous studies have not differentiated between different glial cell types infected in rats (Nagashima et al., 1978, 1979; Koga et al., 1984; Sörensen et al., 1984; Watanabe et al., 1987) and by electron microscopy virus particles were only found in oligodendrocytes (Sörensen et al., 1980). In mice, however, astrocytes were shown to be a target cell for persistent infection (Perlman & Ries, 1987).

*In vitro* results appear to be controversial. Astrocytes were shown to be primary target cells for infection (Massa, Wege & ter Meulen, 1986), but other *in vitro* culture experiments, however, stressed tropism of the virus to oligodendrocytes (Beushausen & Dales, 1985). These differences may be due to the high variability of the virus variants used for infection.

Employing immune electron microscopic techniques, nucleocapsid protein was demonstrated lying free in the cytoplasm and S protein was shown to be associated with perinuclear cisterns, endoplasmic reticulum and vesicles. These findings are compatible with the subcellular distribution of the closely related MHV-A59 strain in cell cultures and with the known fact that coronaviruses bud into intracellular membrane compartments such as endoplasmic reticulum, smooth vesicles and Golgi apparatus (Tooze, Tooze & Warren, 1984). Furthermore, we found evidence that JHM S protein is expressed on the cell surface membrane of infected glial cells *in vivo*. Thus, spike protein is accessible to the humoral immune system. MHV-JHM infected rats generally do show a high virus specific (neutralizing) antibody response in the serum in the late phases of the disease (Koga *et al.*, 1984; Wege *et al.*, 1984b). Synthesis of antibodies with antiviral and unknown specificities was also shown to occur within the brain compartment (Sörensen *et al.*, 1984; Dörries *et al.*, 1986, 1987). Consequently, it is conceivable that during stages of the disease which involve damage to the blood-brain barrier, infected cells might be destroyed through antibody-complement mediated cytotoxity or by antibody dependent cell mediated cytotoxity (ADCC). Furthermore, recent immunosuppression studies have demonstrated that demyelination is not just simply due to cytolytic infection of oligodendrocytes (Wang *et al.*, 1990). MHC restricted cell mediated immune reaction against viral and myelin antigens may play a role in the establishment of a demyelinating disease (Watanabe *et al.*, 1983; Ehrlich, Matsushima & Stohlman, 1989; Wang *et al.*, 1990). However, the notion that an ADCC mechanism operates (in addition to a cell mediated immune response) is supported by the presence of plasma cells and of granular IgG and C9 deposits in actively demyelinating lesions of SDE. These deposits are similar to those described in co-transfer EAE models, in which lesions are induced by MBP reactive T cells in co-operation with monoclonal antibodies against MOG (Linington *et al.*, 1988, 1989).

The results of several studies imply that during the acute stage of disease, the T cell response plays a pivotal role in virus elimination (Kyuwa & Stohlman, 1990; Williamson & Stohlman, 1990; Körner *et al.*, 1991). Neutralizing, S specific antibodies appear later and are important for subsequent protection. On the other hand, the results from our analysis of SDE lesions suggest that inflammatory demyelination could be the consequence of inefficient virus elimination during the clinically silent acute stage. The outcome of the disease in individual animals may depend on the balance between successful virus elimination, tissue destruction and down-regulation of virus production.

It was observed in this study that the number of cells expressing spike protein is reduced in SDE. The mechanism is unclear, but seems to be complex, as a simple masking or shedding of spike protein from the surface by antibodies would not account for the reduced intracellular expression. It is tempting to speculate that the virus down-regulates spike protein production in an attempt to escape from the immune reaction. In favour of this idea is the finding that in JHM-infected glial cell cultures, the presence of S specific antibodies promotes the establishment of a chronic infection and reduces the relative number of cells displaying S protein (Wege *et al.*, 1989). It has been shown in several viral systems, both *in vivo* and *in vitro*, that there is a reduced expression of glycoproteins on the cell surface during persistent infections relative to the levels during acute infections (Oldstone, 1989).

The virological basis for the variable outcome of infection employing syngenic animals is not yet clear. A number of studies suggest that structural features of the highly variable S protein are an important determinant for neurovirulence and cell tropism (Dalziel *et al.*, 1986; Fleming *et al.*, 1987; Wege, Winter & Meyerman, 1988). Furthermore, under certain conditions, antiviral antibodies appear to modulate the disease from an acute to a chronic form (Buchmeier *et al.*, 1984; Perlman *et al.*, 1987).

In summary, our data suggest that the pathogenetic mechanisms leading to demyelination in coronavirus-induced SDE may be similar to those described in chronic relapsing experimental allergic encephalomyelitis (Lassmann *et al.*, 1988; Linington *et al.*, 1988). Inflammation appears to be initiated and propagated by cellular immune reactions against coronavirus N protein or, in chronic animals, against myelin basic protein (Watanabe *et al.*, 1983). Demyelination and tissue damage may then be augmented by antibodies against S protein expressed on the surface of infected oligodendrocytes and astrocytes.

## ACKNOWLEDGEMENTS

## REFERENCES

Beushausen S. & Dales S. (1985) In vivo and in vitro models of demyelinating disease. IX Tropism and differentiation regulate the infectious process of coronaviruses in primary explants of the rat CNS. *Virology* **141**, 89–101

Blakemore W.F. (1975) Remyelination by Schwann cells of axons demyelinated by intraspinal injection of 6-amino-nicotinamide in the rat. *Journal of Neurocytology* **4**, 745–757

Blakemore W.F. (1978) Observations on remyelination in the rabbit spinal cord following demyelination induced by lysolecithin. *Neuropathology and Applied Neurobiology* **4**, 47–59

Blakemore W.F., Crang A.J. & Curtis R. (1986) The interaction of Schwann cells with CNS axons in regions containing normal astrocytes. *Acta Neuropathologica (Berlin)* **71**, 295–300

Blakemore W.F. & Crang A.J. (1988) Extensive oligodendrocyte remyelination following injection of cultured central nervous system cells into demyelinating lesions in adult central nervous system. *Developmental Neuroscience* **10**, 1–11

Buchmeier M.J., Lewicki H.A., Talbot P.J. & Knobler R.L. (1984) Murine Hepatitis Virus-4 (strain JHM)-induced neurologic disease is modulated in vivo by monoclonal antibody. *Virology* **132**, 261–270

Cheever F.S., Daniels J.B., Pappenheimer A.M. & Bailey O.T. (1949) A murine virus (JHM) causing disseminated encephalomyelitis with extensive destruction of myelin: I. Isolation and biological properties of the virus. *Journal of Experimental Medicine* **90**, 181–194

Dal Canto M.C. & Rabinowitz S.G. (1981) Experimental models of virus-induced demyelination of the central nervous system. *Annals of Neurology* **11**, 109–127

Dalziel R.G., Lampert P.W., Talbot P.J. & Buchmeier M.J. (1986) Site-specific alteration of murine hepatitis virus type 4 peplomer glycoprotein E2 results in reduced neurovirulence. *Journal of Virology* **59**, 463–471

Dörries R., Watanabe R., Wege H. & ter Meulen V. (1986) Murine coronavirus induced encephalomyelitides in rats: analysis of immunoglobulins and virus-specific antibodies in serum and cerebrospinal fluid. *Journal of Neuroimmunology* **12**, 131–142

Dörries R., Watanabe R., Wege H. & ter Meulen V. (1987) Analysis of the intrathecal humoral immune response in Brown Norway (BN) rats, infected with the murine coronavirus JHM. *Journal of Neuroimmunology* **14**, 305–316

Erlich S.S., Matsushima G.K. & Stohlman S.A. (1989) Studies on the mechanism of protection from acute viral encephalomyelitis by delayed-type hypersensitivity inducer T cell clones. *Journal of the Neurological Sciences* **90**, 203–216

Fleming J.O., Trousdale M.D., Brabury J., Stohlman S.A. & Weiner L.P. (1987) Experimental demyelination induced by coronavirus JHM (MHV-4): molecular identification of a viral determinant of paralytic disease. *Microbial Pathogenesis* **3**, 9–20

Herndon R.M., Griffin D.E., McCormick U. & Weiner L.P. (1975) Mouse hepatitis virus-induced recurrent demyelination. *Archives of Neurology* **32**, 32–35

Koga M., Wege H. & ter Meulen V. (1984) Sequence of murine coronavirus induced neuropathological changes in rats. *Neuropathology and Applied Neurobiology* **10**, 173–184

Körner H., Schliephake A., Winter J., Zimprich F., Lassmann H., Sedgwick J., Siddell S. & Wege H. (1991) Nucleocapsid or spike protein specific CD4+ T cells alone protect against coronavirus-induced encephalomyelitis. *Journal of Immunology*, in press

Kyuwa S. & Stohlman S.A. (1990) Pathogenesis of a neurotropic murine coronavirus, strain JHM in the central nervous system of mice. *Seminars in Virology* **1**, 273–280

Lampert P.W., Sims J.K. & Kniazeff A.J. (1973) Mechanism of demyelination in JHM virus encephalomyelitis. *Acta Neuropathologica (Berlin)* **24**, 76–85

Lassmann H., Vass K., Brunner C. & Wisniewski H.M. (1986) Peripheral nervous system lesions in experimental allergic encephalomyelitis. *Acta Neuropathologica (Berlin)* **69**, 193–204

Lassmann H., Brunner C., Bradl M. & Linington C. (1988) Experimental allergic encephalomyelitis: The balance between encephalitogenic T lymphocytes and demyelinating antibodies determines size and structure of demyelinated lesions. *Acta Neuropathologica (Berlin)* **75**, 566–576

Linington C., Bradl M., Lassmann H., Brunner C. & Vass K. (1988) Augmentation of demyelination in rat acute allergic encephalomyelitis by circulating mouse monoclonal antibodies directed against a myelin/oligodendrocyte glycoprotein. *American Journal of Pathology* **130**, 443–454

Linington C., Lassmann H., Morgan B.P. & Compston D.A.S. (1989) Immunohistochemical localisation of terminal complement component C9 in experimental allergic encephalomyelitis. *Acta Neuropathologica (Berlin)* **79**, 78–85

Ludwin S.K. (1980) Chronic demyelination inhibits remyelination in the central nervous system. *Laboratory Investigation* **43**, 382–387

Massa P.T., Wege H & ter Meulen V. (1986) Analysis of murine hepatitis virus (JHM strain) tropism toward Lewis rat glial cells in vitro. Type I astrocytes and brain macrophages (microglia) as primary glial cell targets. *Laboratory Investigation* **55**, 318–327

Nagashima K., Wege H., Meyermann R. & ter Meulen V. (1978) Corona virus induced subacute demyelinating encephalomyelitis in rats: a morphological analysis. *Acta Neuropathologica (Berlin)* **44**, 63–70

Nagashima K., Wege H., Meyermann R. & ter Meulen V. (1979) Demyelinating encephalomyelitis induced by a long-term corona virus infection in rats. *Acta Neuropathologica (Berlin)* **45**, 205–213

Oldstone M.B.A. (1989) Viral persistence. *Cell* **56**, 517–520

Perlman S. & Ries D. (1987) The astrocyte is a target cell in mice persistently infected with mouse hepatitis virus, strain JHM. *Microbial Pathogenesis* **3**, 309–314

Perlman S., Schelper R., Bolger E. & Ries D. (1987) Late onset, symptomatic, demyelinating encephalomyelitis in mice infected with MHV-JHM in the presence of maternal antibody. *Microbial Pathogenesis* **2**, 185–194

Sörensen O., Percy D. & Dales D. (1980) In vivo and in vitro models of demyelinating diseases III. JHM virus infection of rats. *Archives of Neurology* **37**, 478–484

Sörensen O., Coulter-Mackie M.B., Puchalski S. & Dales S. (1984) In vivo and in vitro models of demyelinating disease IX. Progression of JHM virus infection in the central nervous system of the rat during overt and asymptomatic phases. *Virology* **137**, 347–357

Spaan W., Cavanagh D. & Horzinek M.C. (1988) Coronaviruses: structure and genome expression. *Journal of General Virology* **69**, 2939–2952

Tooze J., Tooze S. & Warren G. (1984) Replication of coronavirus MHV-A59 in sac-cells: determination of the first site of budding of progeny virus. *European Journal of Cell Biology* **33**, 281–293

Vass K., Berger M.L., Nowak T.S. Jr., Welch W.J. & Lassmann H. (1989) Induction of stress protein HSP70 in nerve cells after status epilepticus in the rat. *Neuroscience Letters* **100**, 259–264

Waksman B.H. & Reingold S.C. (1986) Viral etiology of multiple sclerosis. Where does the truth lie? *Trends in Neuroscience* **9**, 338–391

Wang F.I., Stohlman S.A. & Fleming J.O. (1990) Demyelination induced by murine hepatitis virus JHM strain (MHV-4) is immunological mediated. *Journal of Neuroimmunology* **30**, 31–41

Watanabe R., Wege H. & ter Meulen V. (1983) Adoptive transfer of EAE like lesions from rats with coronavirus induced demyelinating encephalomyelitis. *Nature (London)* **350**, 150–153

Watanabe R., Wege H. & ter Meulen V. (1987) Comparative analysis of coronavirus JHM induced demyelinating encephalomyelitis in Lewis and Brown Norway rats. *Laboratory Investigation* **57**, 375–384

Wege H., Koga M., Watanabe R., Nagashima K & ter Meulen V. (1983) Neurovirulence of murine coronavirus in JHM temperature sensitive mutants in rats. *Infection and Immunity* **39**, 1316–1324

Wege H., Dörries R. & Wege H. (1984a) Hybridoma antibodies to the murine coronavirus JHM: characterization of epitopes on the peplomer protein (E2). *Journal of General Virology* **65**, 1931–1942

Wege H., Watanabe R. & ter Meulen V. (1984b) Relapsing subacute demyelinating encephalomyelitis in rats in the course of coronavirus JHM infection. *Journal of Neuroimmunology* **6**, 325–336

Wege H., Winter J. & Meyermann R. (1988) The peplomer protein E2 of coronavirus JHM as a determinant of neurovirulence: definition of critical epitopes by variant analysis. *Journal of General Virology* **69**, 87–98

Wege H., Winter J., Körner H., Flory E., Zimprich F. & Lassmann H. (1990) Coronavirus induced demyelinating encephalomyelitis in rats: immunopathological aspects of viral persistency. In *Coronaviruses and their Diseases*, Eds D. Cavanagh and T. Brown, pp 637–645. Plenum Press, New York

Weiner L.P. (1973) Pathogenesis of demyelination induced by a mouse hepatitis virus (JHM virus). *Archives of Neurology* **28**, 298–303

Williamson J.S.P. & Stohlman S.A. (1990) Effective clearance of mouse hepatitis virus from the central nervous system requires both CD4+ and CD8+ T cells. *Journal of Virology* **64**, 4589–4592